Energy 303 (2024) 131844

Contents lists available at ScienceDirect

Energy

journal homepage: www.elsevier.com/locate/energy

Wet cooling tower performance prediction in CSP plants: A comparison between artificial neural networks and Poppe's model

Juan Miguel Serrano [a,*], Pedro Navarro [b], Javier Ruiz [c], Patricia Palenzuela [a], Manuel Lucas [c], Lidia Roca [a]

[a] CIEMAT-Plataforma Solar de Almería-CIESOL, Ctra. de Senés s/n, Tabernas, Almería, 04200, Spain
[b] Technical University of Cartagena, Dr. Fleming, s/n, Cartagena, 30202, Spain
[c] Miguel Hernández University of Elche, Avda. de la Universidad, s/n, Elche, 03202, Spain

ARTICLE INFO

Dataset link: http://dx.doi.org/10.5281/zenodo.10806200

Keywords:
Concentrated solar power
Cooling system
Modelling
Neural networks
Sensitivity analysis

ABSTRACT

The efficiency of Concentrated Solar Power (CSP) plants strongly depends on steam condensation temperatures. Current cooling systems, either wet (water-cooled) or dry (air-cooled), present trade-offs. Wet cooling towers (WCT) optimize performance but raise concerns due to substantial water usage, especially in water-scarce prone locations of CSP plants. Dry cooling conserves water but sacrifices efficiency, specially during high ambient temperatures, coinciding with peak electricity demand. A potential compromise is a combined cooling system, integrating wet and dry methods, offering lower water consumption, improved efficiency and flexibility. Incorporating such systems into CSP plants is of considerable interest, aiming to optimize operations under diverse conditions.

This research focuses on the first step towards this goal; developing static models for WCTs. Two approaches, Poppe and Artificial Neural Networks (ANN), are developed and thoroughly compared in terms of prediction capabilities, experimental and instrumentation requirements, sensitivity analysis, execution time, implementation and scalability.

Both approaches have proven to be reliable, with Poppe providing better results, based on MAPE, for the outlet temperature and water consumption (0.87 % and 3.74 %, respectively) compared to a cascade-forward ANN model (1.82 % and 5.21 %, respectively). However, for the target application, the better execution time favours the use of ANNs.

1. Introduction

Concentrated Solar Power (CSP) plants use mirrors to concentrate the sun's energy to finally drive a turbine that generates electricity. This technology currently represents a minor part of renewable energy generation in Europe. Only approximately 5 GW are installed globally (of which 2.3 GW in Europe are concentrated in Spain). However, the potential for growth is significant given the capability of CSP to provide renewable electricity when needed thanks to in-built energy storage continuing the production even in the absence of sunlight, unlike other renewable technologies that are dependent on the availability of the energy source. Of increasing importance is also their potential application in improving the manageability of the grid, replacing fossil fuel alternatives. Their dispatchability enables plants to respond to peaks in demand, and provide ancillary services to the grid. According to the International Energy Agency forecasts, CSP has a huge potential in the long term, ranging from the 986 TWh by 2030 up to 4186 TWh by 2050 [1], which means that CSP will account for 11% of the electricity generated worldwide and for 4% in the case of Europe.

CSP plants are, in general, located in arid areas, where water is scarce. The efficiency of these plants is highly dependent on the temperature at which the steam is condensed. To date, the conventional systems used to remove excess heat from CSP plants are either wet (water-cooled) or dry (air-cooled). The lowest attainable condensing temperature is achieved in wet cooling systems that depend on the wet-bulb temperature, allowing CSP plants to achieve higher efficiencies. However, this efficiency increase is at the expense of a high cost: excessive water use. Dry cooling systems eliminate the water use but they lead to lower plant efficiencies when the ambient air temperature is high. Those hot periods are often the periods of peak system demand and higher electricity sale price. The combination of the advantages of each of them into an innovative cooling system is thus of great interest. There are different types of innovative cooling systems: those that integrate the dry and wet cooling systems into the same cooling

* Corresponding author.
E-mail address: jmserrano@psa.es (J.M. Serrano).

https://doi.org/10.1016/j.energy.2024.131844
Received 4 December 2023; Received in revised form 3 April 2024; Accepted 27 May 2024
Available online 29 May 2024

Nomenclature

a_V	Surface area of exchange per unit of volume (m^2/m^3)
c	Me correlation parameter
c_p	Specific heat (J/kg K)
dy	Differential of variable y
f	Frequency percentage (%)
h	Enthalpy (J/kg)
h_C	Heat transfer coefficient (W/m^2 K)
h_D	Mass transfer coefficient (kg/m^2 s)
Le	Lewis number ($= h_C/\left(h_D c_{p_{ma}}\right)$)
$\dot{m}$	Mass flow rate (kg/s)
Me	Merkel number
N	Number of data points
n	Me correlation parameter
q	Volumetric flow rate (m^3/h)
R^2	R-squared
T	Temperature (°C)
V	Volume of the transfer region (m^3)
v	Velocity (m/s)
y_i	Measurement variable for the ith data point
$\hat{y}_i$	Estimated value of variable y_i
$\bar{y}$	Mean value of the experimental values
z	Height (m)

Greek symbols

ϕ	Relative humidity (%)
ω	Humidity ratio (kg/kg)

Subscripts and superscripts

a	Air
∞	Ambient
fan	Fan
i	Inlet
$lost$	Consumption
o	Outlet
s	Saturated
w	Water
b	Wet bulb

Abbreviations

ACC	Air Cooled Condenser
ANN	Artificial Neural Network
CF	Cascade-forward
CSP	Concentrated Solar Power
Exp	Experimental campaign
FF	Feedforward
MAPE	Mean Absolute Percentage Error
MIMO	Multiple Inputs–Multiple Outputs
NDWCT	Natural Draft Counter-flow Wet Cooling Towers
PSA	Plataforma Solar de Almería
RBF	Radial-basis function
RMSE	Root Mean Square Error
WCT	Wet Cooling Tower
MAE	Mean absolute Error

device, which are called hybrid cooling systems and those that combine separate dry and wet cooling systems, which are called combined cooling systems. In the case of hybrid cooling systems, the dry section are composed of compact heat exchangers included in a wet cooling tower [2]. This kind of cooling systems can be considered as an efficient cooling solution for CSP plants [3] due to the energy conservation and water and greenhouse gas emissions savings. In the case of combined cooling systems, different configurations can be found. The most commonly proposed in the literature is the one that considers an Air Cooled Condenser (ACC) in parallel with a Wet Cooling Tower (WCT), as can be seen in [4,5]. In this kind of configuration, the exhaust steam from the turbine is condensed either through the ACC or through a surface condenser coupled with the WCT. Another configuration, recently proposed in [6] is a wet and a dry cooling tower (type air cooled heat exchanger) sharing a surface condenser. In this case, the exhaust steam from the turbine is condensed through the surface condenser and the heated cooling water is cooled either through the WCT or through the dry cooling tower. This kind of combined cooling systems are proposed as the most suitable option for a flexible operation as a function of the ambient conditions, since they allow to select the best operation strategies to achieve an optimum water and electricity consumption compromise [7]. In addition, if the optimization is combined with energy demand forecasting as described in [8], the expected results can be even better.

In order to perform such optimization, it is first necessary to develop the modelling of the components of this combined cooling system. Since the objective is performance prediction, this paper focuses on the steady state modelling of the WCT. More specifically, the aim is to compare two modelling strategies: that based on physical equations and that based on black box models such as Artificial Neural Networks (ANN), in order to see which one is more suitable for its integration in the optimization of the complete process. In the case of the models based on physical equations, the analysis of wet cooling towers has its origin in [9], in which the theory for their performance evaluation was developed. Merkel proposed a model based on several assumptions to simplify the heat and mass transfer equations to a simple hand calculation. However, these assumptions mean that Merkel's method does not reliably represent the physics of the heat and mass transfer process in a cooling tower. This was already stated by Bourillot [10] who concluded that the Merkel method is simple to use and can correctly predict cold water temperature when an appropriate value of the coefficient of evaporation is used. However, it is insufficient for the estimation of the characteristics of the warm air leaving the fill and for the calculation of changes in the water flow rate due to evaporation. Jaber and Webb [11] developed the equations necessary to apply the effectiveness-NTU method directly to counterflow or crossflow cooling towers. This approach is particularly useful in the latter case and simpler compared to a more conventional numerical procedure. Notice that the effectiveness-NTU method is based on the same simplifying assumptions as the Merkel method. On the other hand, Poppe and Rögener [12] developed the Poppe method. They derived the governing equations for heat and mass transfer in a wet cooling tower and did not make any simplifying assumptions as in the Merkel theory, which makes it a very precise model. As a matter of fact, predictions from the Poppe formulation have resulted in values of evaporated water flow rate that are in good agreement with full scale cooling tower test results [13]. This model has already been used for the evaluation of the thermal performance of solar power plants using different condensation systems (wet, dry and hybrid system), as can be found in Cutillas et al. [14].

In the case of black box models, numerous authors in the literature have designed ANN models for WCT with different objectives, such as performance prediction, simulation and optimization. One of the first works in this area is the one described in [15] where an ANN model was developed to predict the performance of a forced-counter flow cooling tower at lab scale. In this case, the input variables were the

dry bulb temperature, the relative humidity of the air stream entering the tower, the temperature of the water entering the tower, the air volume flow rate and the cooling water mass flow rate. The outputs of this model were the heat rejection rate at the tower, the mass flow rate of water evaporated, the temperature of the cooling water at the tower outlet, the dry bulb temperature and the relative humidity of the air at the outlet of the tower. The results obtained with a 5-5-5[1] ANN demonstrated that wet cooling towers at lab-scale can be modelled using ANNs with a high degree of accuracy. There are also ANN models for Natural Draft Counter-flow Wet Cooling Towers (NDWCT) at lab-scale, such as the one proposed by [16]. In this case, the authors used a 4-8-6 ANN structure and considered some additional variables, such as air gravity, wind velocity, heat transfer coefficients and efficiency as outputs. All these works can be useful to validate the model development methodology but may fail predicting the performance of WCT at larger scale. In this sense, special attention deserves the study carried out by [17] where an 8-14-2 ANN model was proposed to predict the performance (the cooling number and the evaporative loss proportion) of NDWCTs at commercial scale. The model is based on 638 sets of field experimental data collected from 36 diverse NDWCTs used in power plants. It is a very challenging work since it covers samples from a wide range of tower sizes and capacities being the Mean Relative Error (MRE) below 5%.

From the literature review, it can be stated that there are works based on Poppe and ANN models that evaluate the main output variables of WCTs. Nevertheless, to the authors knowledge, there are no studies focused on the comparison between both modelling strategies. Also lacking is a comprehensive analysis of the different aspects that affect the models development and performance.

This paper presents a novel and exhaustive comparison between the two modelling approaches, at steady state and with a focus on optimization applications, in terms of predictive capabilities, experimental and instrumentation requirements, execution time, implementation and scalability. A sensitivity analysis is performed to further analyse and compare each case study. It also presents and evaluates all relevant aspects of interest in the development of such models, specifically for ANNs, model configuration, architecture and topology are discussed. This methodology is applied to a real 200 kW_{th} WCT integrated in a combined cooling pilot plant at the Plataforma Solar de Almería (PSA), for which an extensive experimental evaluation has been carried out to develop and validate both modelling strategies.

The paper is organized as follows: Section 2 contains the description of the experimental facility, the methodology followed to conduct this work, details the two modelling approaches (Poppe and ANNs) and the different experimental campaigns used to evaluate the different modelling approaches as well as the experimental procedure for conducting tests in the pilot plant. In Section 3, individual results are first presented for each modelling alternative followed by a discussion and comparison of them, covering aspects such as: prediction capabilities, experimental data requirements, instrumentation requirements, sensitivity analysis, scalability and performance in diverse conditions, implementation and execution time. Finally, in Section 4 the most important findings and final recommendations of this research are presented.

2. Materials and methods

With the aim of comparing two modelling strategies established to predict the outlet water temperature and the water consumption of WCT (physical equation-based and ANN-based models), three different experimental campaigns have been carried out at the pilot plant of combined cooling systems located at PSA (see a detailed description in Section 2.1): the first one for the calibration of the physical equation-based model, the second one for tuning the ANN-based model and the last one for the validation and comparison of the two modelling strategies. These strategies and the experimental campaigns are exhaustively detailed in Sections 2.3 and 2.4, respectively.

2.1. Description of the pilot plant

The pilot plant of combined cooling systems located at PSA (see the layout in Fig. 1) consists of three circuits: cooling, exchange and heating. In the cooling circuit (see a picture in Fig. 2), water circulating inside the tube bundle of a Surface Condenser (SC) can be cooled through a Wet Cooling Tower and/or a Dry Cooling Tower (type Air Cooled Heat Exchanger, ACHE), both with a designed thermal power of 204 kW_{th}. In the exchange circuit, a saturated steam generator of 80 kW_{th} (on the design point), generates steam at different pressures (in the range between 82 mbar and 200 mbar), which is in turn condensed in the surface condenser. In this way, the steam transfers its latent heat of condensation to the refrigeration water, that is heated. Finally, in the heating circuit, a solar field with a thermal power of 300 kW_{th} at the design point, provides the energy required by the steam generator, in the form of hot water. It is a unique, very flexible, fully instrumented and versatile facility, able to operate in different operation modes: series and parallel mode, conventional dry-only mode (all water flow is cooled through the dry cooling tower) and wet-only mode (all water flow is cooled through the wet cooling tower). The instrumentation related to the WCT is described in Table 1. Note that the sensors measuring the air velocity and temperature and relative humidity at the outlet area of the wet cooling tower have not been installed in the plant. Portable sensors were used instead in some experiments, as described in Section 2.4.1.

In regards to operational aspects of the system, note that the cooling water and air flow rates at the experimental facility ($\dot{m}_w$, and air, $\dot{m}_a$, respectively), are modified with the *Pump 1* and the fan frequency percentage SC-001, respectively (see Fig. 1).

2.2. Methodology

Fig. 3 schematically shows the procedure followed for the calibration, tuning and validation of the two modelling strategies established as well as for the comparison between them.

As previously mentioned, three experimental campaigns have been performed, shown in Fig. 3 as *Exp 1*, *Exp 2*, and *Exp 3*. *Exp 1* corresponds to the Poppe model calibration campaign and it was designed for the calibration of the first principles model. The aims of such campaign was to fit a function (mapping) that relates the air mass flow rate at the outlet of the tower, $\dot{m}_a$, with the frequency of the fan, f_{fan}, and to calibrate a WCT performance coefficient: the Merkel number, Me. Exp 2, which corresponds to the ANN tuning experimental campaign, is a set of data obtained over several years of operation in a wide range of operating and ambient conditions that has been used for tuning the ANN model. Finally, in the validation and comparison experimental campaign (Exp 3), new data, not included in the other two campaigns, has been collected by applying a design of experiments in order to validate and compare the proposed modelling strategies.

To evaluate the quality of the models fit to the experimental data, four performance metrics were evaluated: coefficient of determination (R^2), Root Mean Square Error (RMSE), Mean Absolute Error (MAE) and Mean Absolute Percentage Error (MAPE). These metrics are described below.

Coefficient of determination. R^2 measures the proportion of the variance in the predicted variable that can be attributed to the independent variable(s), in this case the considered system inputs. Values close to one indicate a better prediction accuracy. It is calculated as follows:

$$R^2 = 1 - \frac{\sum_{i=1}^{n}(y_i - \hat{y}_i)^2}{\sum_{i=1}^{n}(y_i - \bar{y})^2},$$

[1] The notation n_1-...-n_l represents the architecture of the ANN model, where l is the number of layers and n_i are the nodes in each one of the layers.

Table 1
Characteristics of instrumentation.

Measured variable	Instrument	Range	Measurement uncertainty
Water temperature (TT-001, TT-006)	Pt100	0–100 °C	0.03 + 0.005·T[a]
Cooling water flow rate (FT-001)	Vortex flow meter	9.8–25 m^3/h	±0.65% o.r.[b]
Water flow rate (FT-004)	Paddle wheel flow meter	0.05–2 m^3/h	±0.5% of F.S[c] +2.5% o.r
Ambient temperature	Pt1000	−40–60 °C	±0.4@20 °C
Relative humidity	Capacitive sensor	0%–98%	±3% o.r @20 °C
Air velocity	Impeller anemometer	0.1–15 m s^{-1}	±0.1 m s^{-1} + 1.5% o.r
Outlet air temperature	Pt100	−20–70 °C	±0.5 °C
Outlet air humidity	Capacitive sensor	0–100%	±2%

[a] Value of the temperature in °C.
[b] Of reading.
[c] Full scale.
[d] Mean value.

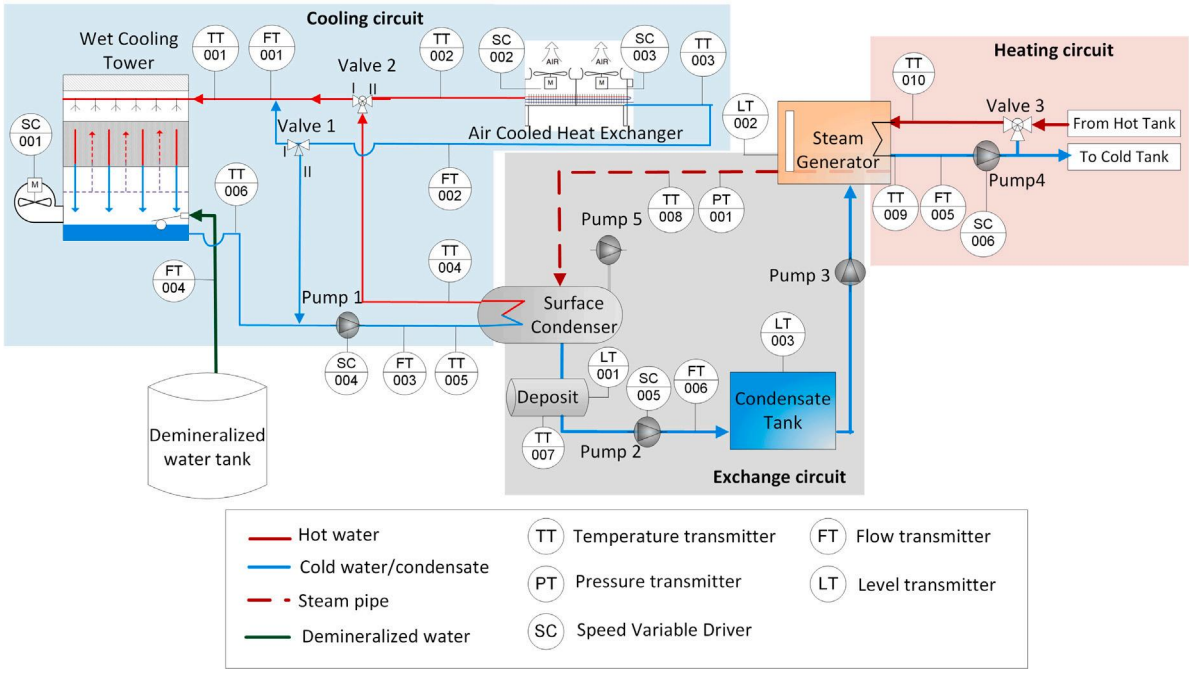

Fig. 1. Layout of combined cooling systems pilot plant at PSA.

where y_i is the measured or observed value for the output variable, in the ith observation, $\hat{y}_i$ is the estimated value of the same variable and n is the total number of observations. Finally, $\bar{y}$ is the mean value of the experimental values.

Root Mean Square Error. RMSE is a statistical measure of the difference between the values predicted by a model and the observed values. It is calculated as the square root of the mean of the squared differences between the predicted and observed values and it has its units.

$$\mathrm{RMSE} = \sqrt{\frac{1}{n}\sum_{i=1}^{n}(y_i - \hat{y}_i)^2}$$

Mean Absolute Error. It represents the average absolute difference between predicted and actual values.

$$\mathrm{MAE} = \frac{1}{n}\sum_{i=1}^{n}\left|y_i - \hat{y}_i\right|$$

Mean Absolute Percentage Error. As the MAE, it calculates the difference between the predicted and the actual values, but in this case it does so in relative terms:

$$\mathrm{MAPE} = \frac{1}{n}\sum_{i=1}^{n}\left|\frac{y_i - \hat{y}_i}{y_i}\right| \times 100\%$$

On the other hand, the robustness and reliability of the models have been evaluated by a sensitivity analysis. It involves systematically assessing how variations in input parameters impact the model's outputs. In this case, the Sobol method [18], which is a variance-based approach, has been used. This method decomposes the total variance of the model output into contributions from individual input parameters and their interactions. By quantifying the relative importance of each parameter, Sobol analysis facilitates the identification of influential factors, enabling a more nuanced understanding of complex systems characterized by numerous interacting variables (five in this case). Sobol sensitivity analysis provides a quantitative basis for assessing the consistency and validity of results when different approaches to model a system are compared. ANNs models with similar sensitivity analysis outcomes to those of the physical model, are likely to capture the essential features of the system, offering a means to verify their credibility and ensuring that the proposed solutions align with the underlying physical principles. Therefore, Sobol sensitivity analysis emerges as a powerful tool not only for understanding the system

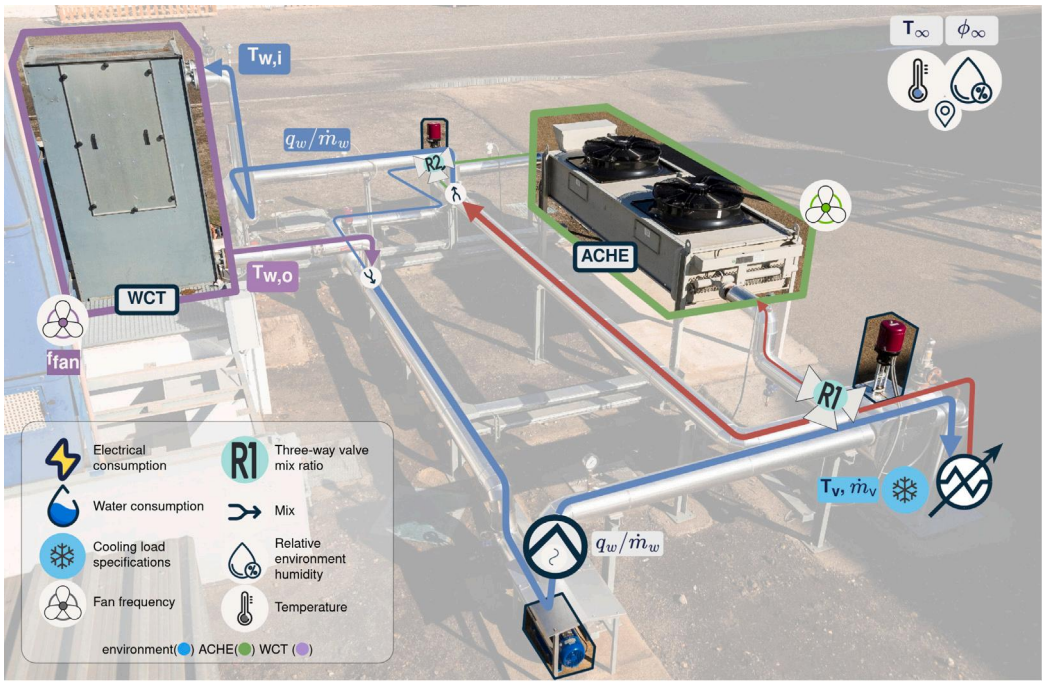

(a) The cooling circuit

(b) Back view of the WCT

Fig. 2. Pictures of the combined cooling pilot plant at PSA.

input–outputs relationships, but also as a way to validate and compare various modelling approaches. The sensitivity analysis has been performed using *SAlib*, an open source sensitivity analysis tool for the Python programming language [19,20].

2.3. Modelling

The static models presented in this section have been developed to predict two main outputs, the water temperature at the outlet of the WCT, $T_{w,o}$, and the water consumed due to evaporation losses, $\dot{m}_{w,lost}$. The inputs variables required by both modelling approaches, Poppe model and ANN models, are: the cooling water flow rate ($\dot{m}_w$), the water temperature at the inlet of the WCT ($T_{w,i}$), the ambient temperature (T_∞), the ambient relative humidity (ϕ_∞) and the frequency percentage of the fan (f_{fan}) (or its equivalence in air mass flow rate,[2] $\dot{m}_a$).

[2] ANN uses as input f_{fan} whereas Poppe's model uses $\dot{m}_a$.

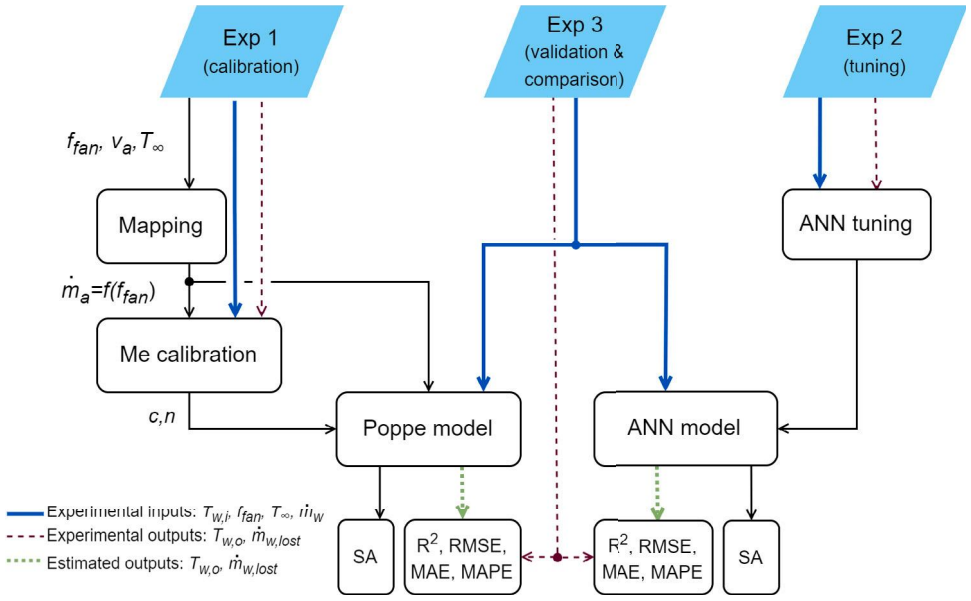

Fig. 3. Calibration, tuning, validation and comparison procedure.

$$\frac{d\omega}{dT_w} = \frac{c_{p_w}\frac{\dot{m}_w}{\dot{m}_a}\left(\omega_{s,w}-\omega\right)}{\left(h_{s,w}-h\right)+(\mathrm{Le}-1)\left[\left(h_{s,w}-h\right)-\left(\omega_{s,w}-\omega\right)h_v\right]-\left(\omega_{s,w}-\omega\right)h_w} \tag{2}$$

$$\frac{dh}{dT_w} = c_{p_w}\frac{\dot{m}_w}{\dot{m}_a}\left[1+\frac{\left(\omega_{s,w}-\omega\right)c_{p_w}T_w}{\left(h_{s,w}-h\right)+(\mathrm{Le}-1)\left[\left(h_{s,w}-h\right)-\left(\omega_{s,w}-\omega\right)h_v\right]-\left(\omega_{s,w}-\omega\right)h_w}\right] \tag{3}$$

$$\frac{d\,\mathrm{Me}}{dT_w} = \frac{c_{p_w}}{\left(h_{s,w}-h\right)+(\mathrm{Le}-1)\left[\left(h_{s,w}-h\right)-\left(\omega_{s,w}-\omega\right)h_v\right]-\left(\omega_{s,w}-\omega\right)h_w}, \tag{4}$$

Box I.

2.3.1. Poppe model

The well-known Merkel number is accepted as the performance coefficient of a wet cooling tower [21]. This dimensionless number is defined in Eq. (1), and it measures the degree of difficulty of the mass transfer processes occurring in the exchange area of a wet cooling tower.

$$Me = \frac{h_D a_v V}{\dot{m}_w}, \tag{1}$$

where h_D is the mass transfer coefficient, a_V is the surface area of exchange per unit of volume and V is the volume of the transfer region, as described in the Nomenclature Section.

The Merkel number can be calculated using the Merkel and Poppe theories for the performance evaluation of cooling towers. On the one hand, the Merkel theory [9] relies on several critical assumptions, such as the Lewis factor (Le) being equal to 1, the air exiting the tower being saturated with water vapour and it neglects the reduction of water flow rate by evaporation in the energy balance. On the other hand, the Poppe theory [12], which is the one used in this work, do not consider simplifying assumptions, thus being the one most usually preferred. In this theory, the authors derived the governing equations for heat and mass transfer in the transfer region of the wet cooling tower (control volume shown in Fig. 4) assuming a one dimensional problem. In this figure, the red and green dashed lines indicate the fill and air-side control volumes, respectively.

Following the detailed derivation process and simplification of the previously-mentioned governing equations described in [21], the major following equations for the heat and mass transfer obtained, according to the Poppe theory, are: (see the Eqs. (2)–(4) in Box I), where the quantity referred to as Me in Eq. (4), is the Merkel number calculated according to the Poppe theory. The above described governing equations can be solved by the fourth order Runge–Kutta method to provide the evolution of the air humidity ratio, air enthalpy and Merkel number inside the transfer area of the cooling tower (fill). Once these profiles

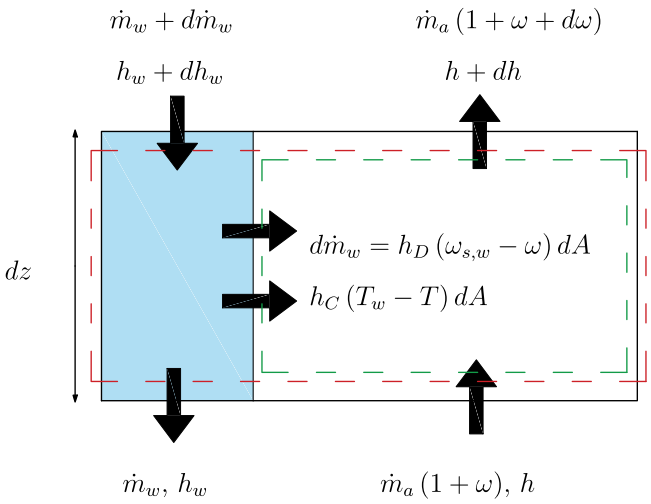

Fig. 4. Control volume in the exchange area of a wet cooling tower for counterflow arrangement.

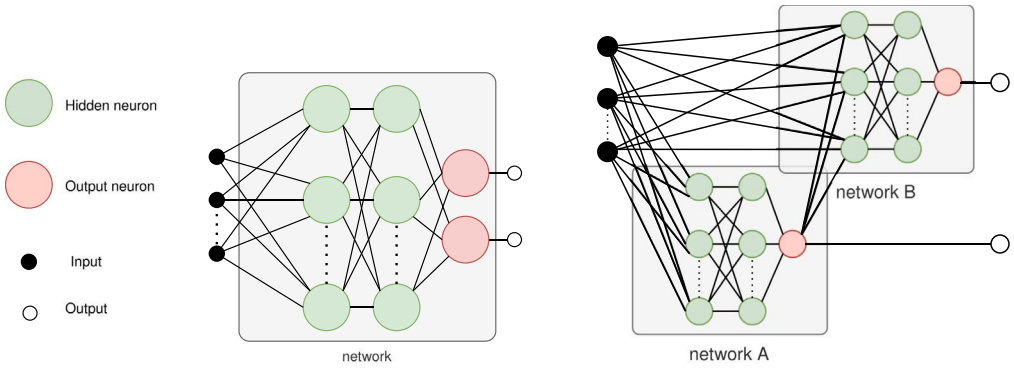

(a) MIMO configuration (b) Cascade configuration

Fig. 5. ANN model configurations considered.

are known, the amount of water lost due evaporation can be calculated as per Eq. (5). Refer to [21] for additional information concerning the calculation procedure.

$$\dot{m}_{w,lost} = \dot{m}_a(\omega_{a,o} - \omega_{a,i}) \tag{5}$$

It is important to mention that the Merkel number varies with the operation conditions and its value can be obtained using a correlation with the water-to-air mass flow ratio as an independent variable. One of the proposed correlations in ASHRAE [22] is: $\mathrm{Me} = c\left(\dot{m}_w/\dot{m}_a\right)^{-n}$, where the constants c and n have been obtained from the fitting of the experimental data, as it is shown in Section 3.2.

2.3.2. Neural network models

Machine learning algorithms are unique in their ability to obtain models and extract patterns from data, without being explicitly programmed to do so. They are more effective with large volumes of data but can also be applied to build steady state regression models with fewer information of a process. Artificial neural networks (ANNs) are part of this set of algorithms and, as the name suggests, have a behaviour similar to biological neurons. Their structure is formed by a succession of layers, each one composed by nodes (or neurons) and they receive as input the output of the previous layer. This process is subsequently repeated until the final layer which has a number of neurons equal to the number of outputs.

There are important aspects to be considered in the ANN model design, such as the model configuration, the network architecture and the network topology. They are discussed below.

Model configuration. The WCT model has two outputs, and thus several configurations are available for the implementation of the model as shown in Fig. 5. The first one is a Multiple Inputs–Multiple Outputs (MIMO) configuration, where a single network receives the five defined inputs and directly produces the two desired outputs. The second one is a cascade structure. This cascading approach involves training a network (*network A* in Fig. 5(b)) to predict the outlet water temperature using the initial five inputs. Subsequently, these inputs, along with the output from the temperature-predicting network, are fed into a second network (*network B* in Fig. 5(b)) that is in charge of forecasting the system's water consumption. A potential advantage of this configuration is that it may reduce the experimental data requirements to obtain satisfactory results.

Network architectures. Three network architectures have been implemented and tested:

1. Feedforward network (FF) - Fig. 6(a). This is the base network architecture, where different layers are added sequentially and the flow of information is unidirectional. The transfer function adopted in the hidden layers is the differentiable *Log-Sigmoid*, whereas the one employed in the output layer is a linear one with no saturations.
2. Cascade-forward network (CF) - Fig. 6(b). It is a variation on the feedforward network since it adds direct connections from the input and hidden layers to the output layer.
3. Radial-basis function network (RBF) - Fig. 6(c). The transfer functions used in the first layer of the RBF network are different, they are local Gaussian like functions. Also, instead of multiplying by the weights, the distance between inputs and weights is computed and the bias is multiplied instead of added [23].

Network topology. Two-layer networks (one hidden and one output layer) can learn almost any input–output relationship, including non-linear ones. Adding more layers can improve the learning for more complex problems. However, increasing the number of layers or neurons per layer increases the training computational requirements, requires more data for a satisfactory model and can lead to overfitting. Therefore, the process is usually started with two layers and then the number of layers is increased if they do not perform satisfactorily [23]. In this study, for the feedforward and cascade-forward architectures, one and two hidden layers have been tested with the following configurations: 5, 10, 20, 5–5, 5–10, 10–5, 10-10. For the case of the RBF, it only has one hidden layer and neurons are added sequentially during the training process up to a maximum which is set to 120 neurons.

Training process. The next important aspect to consider is the training process. For the FF and CF networks many Gradient- or Jacobian-based algorithms can be utilized. In this case, the Levenberg–Marquardt backpropagation algorithm [24] has been used. It is a fast algorithm, ideal for multilayer networks with up to a few hundred weights and biases enabling efficient training. The training in this case is done in batches since sequential training is slower and does not produce better results. All data have been normalized applying the z-score normalization method. The criteria established for deciding when to stop the training is the following one: when the performance on the validation set increases (worsens) or when the gradient is below a minimum (1×10^{-7}) for a number of iterations or epochs, or when a maximum number of 1000 epochs is reached. The number of iterations to wait, often refereed as patience, is set to 6. Finally, the selected network parameters will be those of the best epoch.

For each network architecture, the training process was repeated a total of ten times (this is the recommended practice if the computational requirements allow it, since it guarantees reaching a global optimum with a high degree of confidence [25]). The optimal architecture and training was selected according to a performance function, which in this case has been the Mean Square Error (MSE) with the values normalized.

In the case of the RBF network, the chosen training method consists in two stages which treats the two layers of the RBF network separately. The first layer weights and biases are tuned based on the orthogonal least squares method [23], while for the second layer are computed

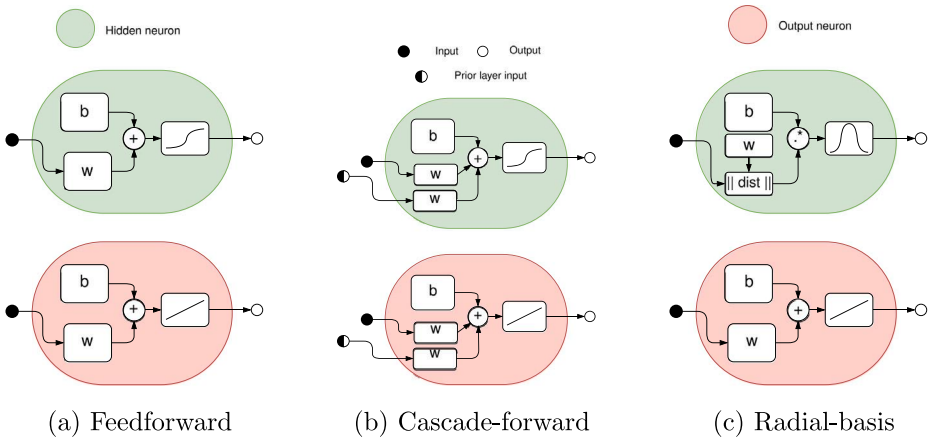

Fig. 6. Considered ANN architectures.

in one step using a linear least-squares algorithm. During training, neurons are added to the first layer (in increments of 20) trying to minimize the MSE to some goal, which in this case is set depending on the case study: 10 for the MIMO configuration and 0 ($°C^2$) and 20 (l^2/h^2) for temperature and water lost networks, respectively, for the cascade configuration. Finally, a parameter called spread is used to set the first layer biases. Larger values of this parameter promote a smoother approximation of the training data (more generalization), conversely, lower values provide a more exact fit to the training data. Values from 0.1 to 30 have been tested for this parameter.

2.4. Experimental campaigns

As mentioned, two modelling approaches have been implemented for performance evaluation of a WCT: the Poppe model (based on physical equations) and ANN-based models (which are data driven). With the aim of calibrating, validating and comparing both modelling strategies, three experimental campaigns have been performed. The set of experimental data obtained with the pilot plant provides a fundamental value to the study carried out and it is one of the strengths of the study performed. A total of 132 steady-state experimental points have been obtained thanks to the thorough experimentation conducted. These data cover a large variety of ambient conditions (different seasons, days and nights) and thermal loads (from 27 kW to 207 kW).

The normative framework followed to carry out the experiments, in order to ensure stable conditions, has been the standards UNE 13741, titled *Thermal Performance Acceptance Testing of Mechanical Draught Series Wet Cooling Towers* [26], and CTI's *Acceptance Test Code for Water Cooling Towers* [27]. These standards specify the test duration and the allowed variations of the most representative ambient and operating magnitudes (water flow rate, heat load, cooling tower range, wet-bulb and dry-bulb temperatures and wind velocity) during the tests. Although the duration of the test should not be less than one hour according to the standards, due to the low capacity of the WCT in the PSA pilot plant and the operational experience, the duration of the tests has been reduced to up to 30 min. Once stable conditions are maintained during the defined interval time, the average and deviations values of each measurement are calculated in order to check that they are within the allowable limits of the norm, which finally lead to a valid steady-state operating point.

2.4.1. Experimental campaign 1 - Exp 1

This campaign was specifically designed for the calibration of the physical model. In total, 19 experimental tests were performed at the combined cooling pilot plant at PSA. The physical model focuses on the calculation of the Merkel number which, according to the literature ASHRAE [22], is not a constant value. Instead, it varies depending on the operating conditions (water-to-air mass flow ratio, $\dot{m}_w/\dot{m}_a$). Therefore, the experimental campaign has been designed to cover different water-to-air mass flow ratios. Both variables, the water and the air flow rates, were varied within the allowable range for plant operation. In the case of the water flow rate, it ranged from 8 m^3/h to 22 m^3/h, and in the case of the air mass flow rate, it was modified by changing the fan frequency from 12.5 Hz to 50 Hz (fan frequency percentage, f_{fan}, from 25% to 100%). The magnitudes required to experimentally determine the air mass flow rate (air velocity and air temperature and relative humidity) were measured at the outlet area of the cooling tower with the sensors listed in Table 1. The outlet area was divided into 9 quadrants and the above mentioned magnitudes were registered at the centre of each quadrant. The obtained values were averaged to determine the mean velocity, temperature and relative humidity used in the air mass flow rate calculation.

As the measurements for the air mass flow rate are a specific requirement for the Poppe model, the $\dot{m}_a - f_{fan}$ relationship shown in Eq. (6) was also derived during this experimental campaign. Following the same experimental procedure described earlier, air velocity, temperature and humidity maps were measured for 8 different f_{fan} levels (ranging from 30% to 100% in 10% intervals). This correlation enables the calculation of the air mass flow rate using the permanent sensors installed in the facility.

$$\dot{m}_a = -0.0014 f_{fan}^2 + 0.1743 f_{fan} - 0.7251. \tag{6}$$

2.4.2. Experimental campaign 2 - Exp 2

The data required for an ANN model depend on several factors such as the complexity of the model and the error allowed or the diversity of the inputs. With the aim of obtaining a reliable ANN model for the WCT, data collected over several years of operation of the combined cooling system have been used for tuning. They are a set of 115 stationary data covering the following operating ranges: ambient temperature, T_∞, [9–39] °C, ambient humidity, ϕ_∞, [10–87]%, inlet water temperature, $T_{w,i}$ [33–41] °C, cooling water flow rate, q_w, [6–23] m^3/h and fan frequency percentage, f_{fan} [21–94]%. The thermal load in these tests varies in the range of [27–178] kW_{th}. The number of steady-state data used is a reasonable value when compared to other similar ANN models of counter-flow cooling towers, as in the case of [15], where 81 experimental points were collected for training and testing.

2.4.3. Experimental campaign 3 - Exp 3

With the aim of validating and comparing both models, a dataset of 17 tests (different from the ones taken for experimental campaigns 1 and 2) has been used. This experimental campaign was designed using a design of experiments based on full factorial design with 4 factors and 2 levels (low and high), whose values are shown in Table 2.

Table 2
Design of experiments for model comparison.

Variable	Low level	High level
T_b (°C)	≤10	≥15
$T_{w,i}$ (°C)	≤37	≥39
$\dot{m}_w$ (kg/s)	≤3.3	≥5
$T_{w,i} - T_{w,o}$ (°C)	≤7	≥8

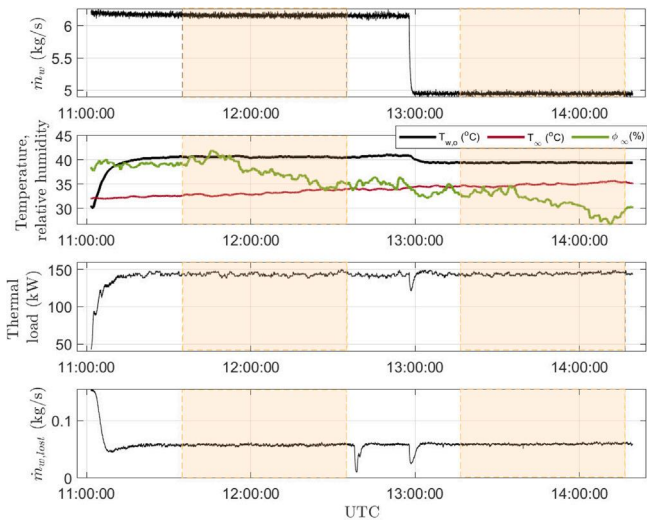

Fig. 7. Example of one experiment at PSA pilot plant (July with two valid steady-state operating points).

An additional test at design operating conditions of the WCT ($T_{b,\infty}$ = 21 °C, $T_{w,i}$ = 40 °C, $\dot{m}_w$ = 6.9 kg/s and $T_{w,i} - T_{w,o}$ = 7 °C) has been also included in this test campaign, where $T_{b,\infty}$ is the ambient wet bulb temperature and $T_{w,o}$ the temperature of the water at the outlet of the WCT.

3. Results

This section firstly shows an example of one experiment at the PSA pilot plant to visualize how the steady state values included in the different data sets are calculated. Then, the results obtained with the two modelling approaches are analysed, and finally a comparison and discussion is presented.

3.1. Experimental tests performed at PSA pilot plant

Fig. 7 shows the main variables involved in one of the experiments performed at the pilot plant at constant air flow rate (f_{fan} = 25%). As can be observed, there are two time intervals in this case, in which the process is at stationary conditions according to the normative framework mentioned in Section 2.4. In order to process the results of the experimental tests and identify valid time intervals, such as the ones shown in this example, a function has been implemented in the Matlab environment. This function identifies whether the standard criteria is met and calculates the mean values of the required variables.

3.2. Poppe model

Table 3 shows the average values of the variables required to calculate Me, which were obtained from Exp 1. As can be observed, the range of air and water mass flow rates are 1.16–4.32 kg/s and 2.17–6.15 kg/s, respectively. Regarding the environmental conditions, these were quite similar for all tests: high ambient temperatures (ranging between 32 °C and 41 °C), and low ambient relative humidities (between 13 % and 40 %) since the experiments were carried out during the summer season.

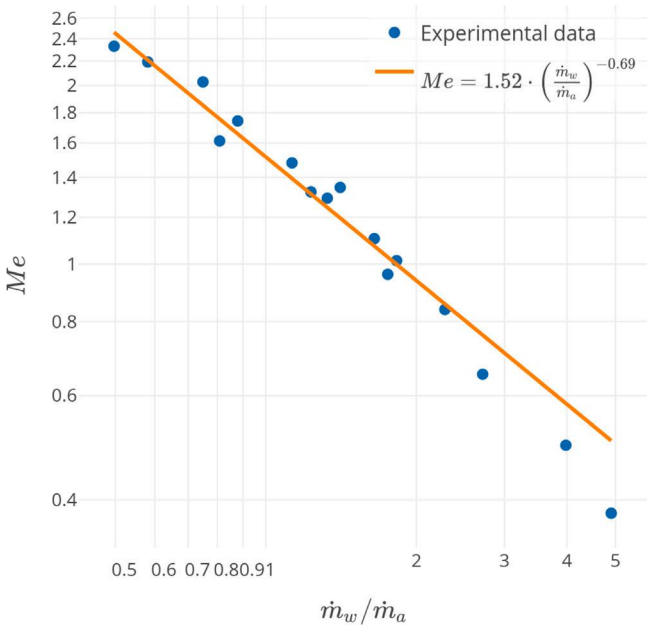

Fig. 8. Experimental results for the Me number as a function of $\dot{m}_w/\dot{m}_a$.

Fig. 8 shows the variation of the Merkel number as a function of the water-to-air mass flow ratio ($\dot{m}_w/\dot{m}_a$) using the data shown in Table 3. As can be seen, the Me decreases with $\dot{m}_w/\dot{m}_a$ values following a linear trend on log–log scale.

Following the correlation for the Merkel number of a wet cooling tower described in Section 2.3.1, the parameters c and n obtained from the data fitting are 1.516 and 0.693, respectively.

3.3. ANN models

When tuning a neural network, the data is divided into two distinct sets. The first one is the training set and it is used to tune the network parameters. The second one is the evaluation set and it is used to evaluate the quality of the ANN. In the case of FF and CF models, the evaluation of the training stop criteria is performed with this second set. In the case of the RBF implementation, the evaluation set is used to select the best spread. For this study, one random division of the data available in Exp 2 has been made, and used to tune the alternatives. The dataset consists on 115 points, of which 80% was assigned to the first set (92 points) and 20% to the second one (23 points).

As mentioned in the *Methodology* Section 2.3.2, two different model configurations are tested with three different network architectures, resulting in 6 distinct models. The best topology obtained for each alternative can be seen in Table 4 - *Topology*,[3] where best is defined in terms of performance metric value for the evaluation set (20% of Exp 2). MIMO feedforward networks favour the use of a single hidden layer (20-2), and two in the cascade configuration, while cascade-forward networks make use of two hidden layers in both configurations. In the case of the RBF there is a clear trend, where the cascade temperature predicting network uses the most neurons (92) and the water loss one the least (29). It follows that the MIMO configuration is somewhere in between with 37. This trend continues on the spread values, where lower values are optimal when more neurons are present (10.78 for $T_{o,w}$

[3] In Table 4, when *Model config* is MIMO, the topology for the outlet temperature and water loss is the same since it is the same network.

Table 3
Averaged values obtained from the experiments performed in Exp 1.

Test	f_{fan} (Hz)	T_∞ (°C)	ϕ_∞ (%)	T_{b_∞} (°C)	$T_{w,i}$ (°C)	$T_{w,o}$ (°C)	$T_{a,o}$ (°C)	$\dot{m}_a$ (kg s^{-1})	$\dot{m}_w$ (kg s^{-1})
1	12.5	33.31	39.58	22.53	48.88	34.79	46.32	1.193	2.173
2	25	34.60	30.41	21.34	44.64	27.97	38.04	2.623	2.170
3	37.5	34.11	38.58	22.92	44.43	26.51	34.73	3.666	2.169
4	50	36.02	29.94	22.23	43.74	25.43	34.97	4.248	2.170
5	12.5	40.50	13.11	19.97	46.85	36.94	49.64	1.157	3.263
6	25	39.75	12.97	19.50	40.30	28.42	39.92	2.588	3.272
7	37.5	36.93	22.39	20.79	38.13	26.25	35.51	3.648	3.266
8	50	35.79	16.13	18.24	35.34	23.32	32.33	4.319	3.268
9	12.5	34.69	32.55	21.94	46.53	39.44	47.83	1.177	4.895
10	25	33.57	27.24	19.83	38.37	30.15	38.25	2.619	4.914
11	37.5	35.66	25.14	20.71	35.39	27.57	35.94	3.637	4.942
12	50	33.53	29.29	20.30	34.50	26.27	33.36	4.292	4.940
13	12.5	32.84	38.77	21.99	46.25	40.57	46.99	1.186	6.096
14	25	34.25	16.50	17.42	36.41	29.81	39.49	2.596	6.127
15	37.5	35.99	16.91	18.59	33.54	27.04	35.38	3.651	6.133
16	50	35.80	14.73	17.83	31.30	24.87	32.99	4.302	6.147

Table 4
Summary table of the prediction results obtained with the different modelling approaches studied.

Predicted variable	Modelling alternative	Model config	Topology	Performance metric								Evaluation time (s)
				R^2 (–)		RMSE (s.u.)		MAE (s.u.)		MAPE (%)		
				T	V	T	V	T	V	T	V	
$T_{o,w}$ (°C)	Poppe	–	–	–	0.98	–	0.33	–	0.27	–	0.87	6.288
	Feedforward ANN	MIMO	20-2	0.93	0.89	0.52	0.74	0.37	0.51	1.22	1.78	0.004
	Cascade-forward ANN	MIMO	10-5-2	0.93	0.90	0.50	0.70	0.35	0.47	1.15	1.65	0.004
	Radial basis ANN	MIMO	37-2	0.99	0.95	0.23	0.51	0.18	0.40	0.57	1.35	0.004
	Feedforward ANN	Cascade	10-10-1	0.94	0.89	0.46	0.72	0.32	0.49	1.05	1.71	0.007
	Cascade-forward ANN	Cascade	10-10-1	0.94	0.87	0.46	0.79	0.31	0.52	1.02	1.82	0.008
	Radial basis ANN	Cascade	92-1	0.99	0.69	0.23	1.22	0.08	0.92	0.25	3.20	0.008
$\dot{m}_{w,lost}$ (l/h)	Poppe	–	–	–	0.97	–	8.47	–	6.74	–	3.74	6.288
	Feedforward ANN	MIMO	20-2	0.95	0.90	11.75	16.27	9.47	14.53	7.74	8.44	0.004
	Cascade-forward ANN	MIMO	10-5-2	0.96	0.94	10.52	12.68	8.23	10.96	6.68	6.33	0.004
	Radial basis ANN	MIMO	37-2	0.99	0.93	4.88	13.86	3.67	10.93	2.94	6.76	0.004
	Feedforward ANN	Cascade	20-1	0.97	0.93	9.64	13.57	7.50	11.18	6.12	6.39	0.007
	Cascade-forward ANN	Cascade	10-10-1	0.97	0.95	8.52	11.24	6.18	9.15	4.92	5.21	0.008
	Radial basis ANN	Cascade	29-1	0.98	0.91	7.63	15.70	4.54	12.41	4.13	6.93	0.008

compared to 27.86 for $\dot{m}_{w,lost}$ in the cascade configuration). This trend is a consequence of the chosen MSE goals during the training process (see Section 2.3.2).

On the other hand, Fig. 9 shows the results obtained with each ANN alternative. It shows the perfect fit together with the results obtained with the MIMO feedforward (a), cascade CF (b) and MIMO radial-basis (c) alternatives. Comparing the feedforward (a) and the cascade-forward (b) cases, it can be seen that their responses are almost identical for the temperature prediction, with about 0.5 °C of RMSE in both data sets. The radial-basis network outperforms both networks for this output in the training set (RMSE = 0.2 °C), but more importantly, in the evaluation set with a value of 0.3 °C. Focusing on the water loss predictions, once again the RBF network shows the best performance (6.4 l/h), followed by the MIMO FF (10.5 l/h) and finally the Cascade CF (13.2 l/h).

It should be noted that this analysis is based on data from Exp 2, in the following section, more meaningful results are analysed since they are based on Exp 3, which contains new data unseen during the training process, and thus it guarantees independent results. The important thing to take from these results, is that there are no significant differences between the train and evaluation sets, which indicates a satisfactory training.

3.4. Discussing the two modelling approaches

In this section, the results obtained from each modelling approach are compared in terms of several aspects: their prediction capabilities, the experimental requirements to develop the models, their sensitivity response to the different inputs, scalability and other practical aspects such as ease of implementation and computational requirements.

3.4.1. Prediction capabilities

The results of each modelling alternative and its comparison can be visualized in Fig. 10 and Table 4. Fig. 10 shows the results obtained with the models using Exp 3. It shows the perfect fit together with the results obtained with Poppe's model, MIMO FF, cascade CF, and MIMO RBF. In Table 4, the performance of the studied modelling approaches are included for the different performance metrics (described in Section 2.2). *T* represents the performance metric value for the training/calibration dataset (Exp 1 or Exp 2 depending on the case), and V for the validation and comparison one (Exp 3). In all cases the model representing each alternative is in the best case scenario, i.e. maximum number of points available. On the other hand, s.u. indicates that the units of the column are the same as from the source variable.

Comparing both modelling approaches (see Fig. 10), it can be outlined that both models provide a good prediction of the output variables, falling most of the discrepancies (errors) within the uncertainty range. Poppe's model provides a better prediction of the outlet temperature, obtaining an RMSE of 0.33 °C and an R^2 of 0.98. In comparison, the best ANN alternative (RBF MIMO) has a slight worse performance with an RMSE of 0.51 °C and R^2 = 0.95. In terms of water consumption, the physical model has a better prediction accuracy in terms of RMSE and R^2 (8.5 l/h and 0.97) compared to 11.24 l/h and 0.95 for the best ANN model (cascade CF). It can be stated that, although the results are better for the physical model (specially in the

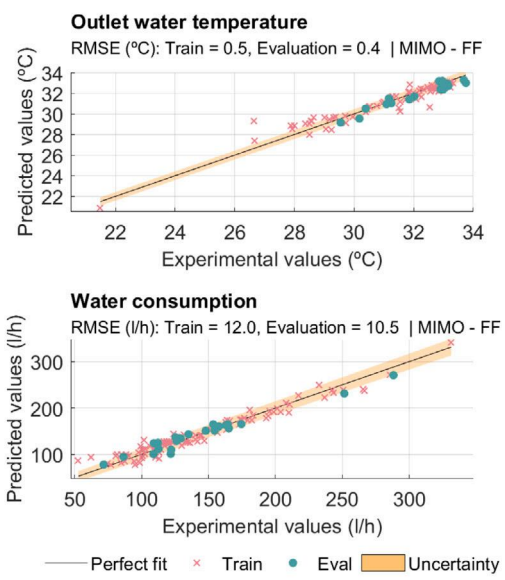

(a) MIMO FF model

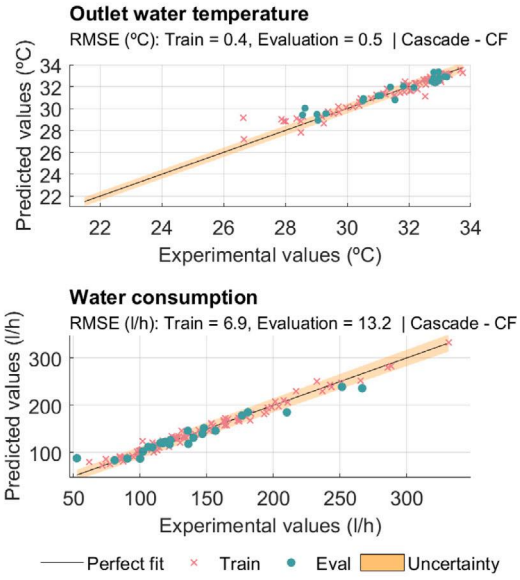

(b) Cascade CF model

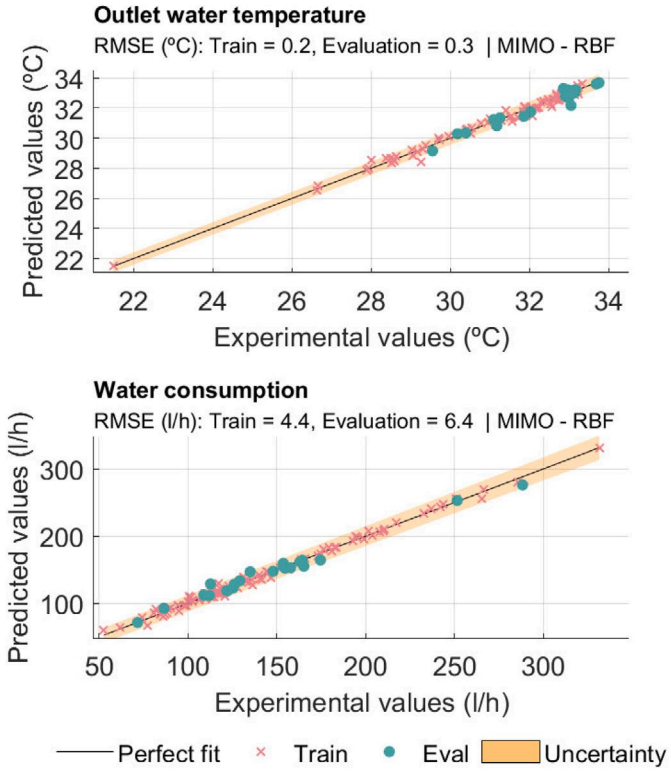

(c) MIMO RBF model

Fig. 9. ANN regression model results with Exp 2 in best case scenario.

case of the outlet temperature prediction), both approaches produce valid results with high accuracy levels.

3.4.2. *Experimental data requirements*

In order to estimate the minimum number of tests required to obtain satisfactory results with both modelling strategies, an analysis was performed in which each modelling alternative was calibrated/tuned for different case studies with different amounts of available data, and then the performance metrics were evaluated. In this way, trends in the predictive accuracy of the models as a function of the available data can be identified. When the variation becomes small, it can be stated that the model has converged and adding more information provides diminishing returns.

For the physical model, the number of tests from Exp 1, used to calibrate Me correlation, was varied from 2 up to 16 data points added sequentially. In the case of the ANN models, the available tuning data (Exp 2) was increased in steps of 10%, starting from the availability of 10% up to the entire data set (100%).

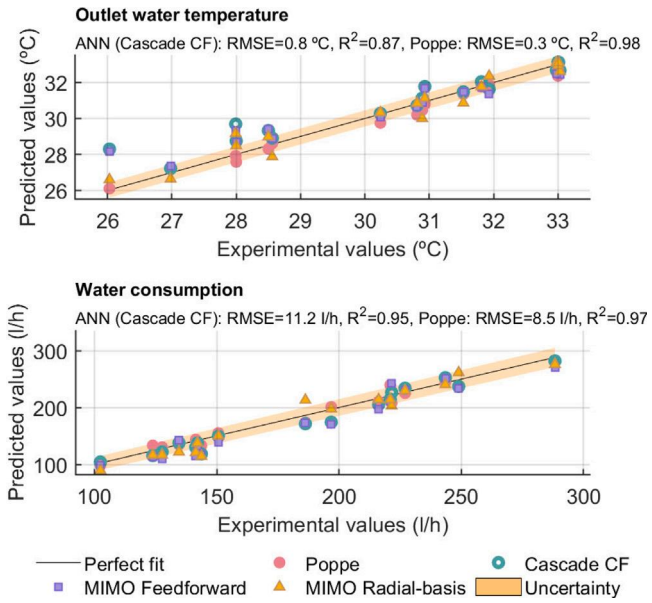

Fig. 10. Model results obtained with Poppe and ANN models and data of Exp 3.

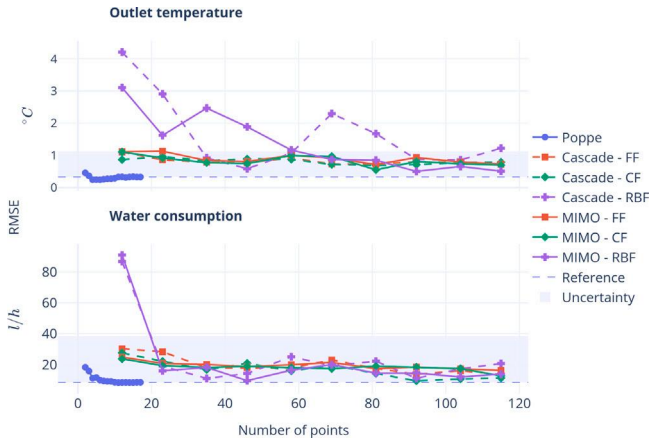

Fig. 11. Root Mean Square Error (RMSE) evolution as a function of the number of points used for calibration/training of the Poppe's and ANN approaches.

In both cases, the criteria for selecting the data was not random, but it was done by applying physical knowledge. The water-to-air mass flow ratio, $\dot{m}_w/\dot{m}_a$, is a good indicator for selecting the operation points to be fed to the model. The trend observed in Fig. 8 (decreasing Me for increasing $\dot{m}_w/\dot{m}_a$) has been extensively reported in the literature. This behaviour is explained by the increase in the amount of water per unit of air that lead to a less effective cooling [28]. The situation corresponding to the minimum $\dot{m}_w/\dot{m}_a$ can be interpreted as the maximum air flow rate for a given water flow rate to be cooled. This results in the maximum driving force and, therefore, maximum Merkel number. As $\dot{m}_a$ decreases progressively, the driving force decreases for a given $\dot{m}_w$, and Me decreases accordingly. Based on this knowledge, the selection starts by choosing extreme points for the water-to-air mass flow ratio in the Me-$\dot{m}_a/\dot{m}_w$ relationship from the available data, which gives information of the system operating in its limits. Subsequently intermediate points are added, covering this way the whole operating range of the cooling system.

The results of this study are presented in Fig. 11, where the x-axis represents the number of available data points and the y-axis a model performance metric (RMSE) obtained when the model outputs are compared to data from Exp 3. From the results obtained, it can be clearly seen the advantage of the physical model in terms of data requirements, since with the minimal amount of points, good results are obtained, and by enlarging the available data points to 8–10, low variation in the RMSE evolution can be observed for both predicted variables. In the case of the ANN-based approaches, the results differ depending on the ANN alternative.

In terms of the outlet temperature, very good results (low error and variation) are obtained with the minimal dataset (10% of available data, 12 data points) for feedforward and cascade-forward in any configuration (MIMO and cascade). If more data is added, RMSE is reduced from 1.1 up to 0.7 °C. Although the MIMO RBF outperforms the results of the other ANN alternatives, it does so only from 90 points onwards. For this case, the downward trend is much more noticeable but constant, which cannot be stated for the cascade RBF, displaying an erratic evolution up to 70 points.

Similar conclusions can be drawn for the water consumption, except that in this case the two RBF configurations achieve satisfactory results much earlier, starting from 23 points.

Summarizing, both modelling approaches, Poppe's model and ANNs, produce satisfactory results since their predictions fall well within the range of uncertainty for all the case studies, although the obtained results, in terms of RMSE, favour the physical model. Therefore, while the ANN model benefits from as much data as possible, the Poppe model is already able to produce satisfactory results with just two properly selected points. These two points are easy to identify in advance because they are related to the maximum and minimum $\dot{m}_w/\dot{m}_a$ ratio of the wet cooling tower. In practice, to minimize the error prediction, around 5 points are often used. Out of the ANN alternatives, considering both output variables, if less than 70 data points are available, cascade-forward and feedforward alternatives with any configuration are the best option, producing satisfactory results with as low as 10 points. On the other hand, if enough data is available, MIMO RBF should be considered as a strong candidate, but not in the cascade configuration alternative.

3.4.3. Instrumentation requirements

Another important consideration is the instrumentation requirements. Poppe's model requires measurements of the airflow at the outlet of the WCT, while the ANN model can use the frequency of the WCT fan directly as an input.

This measurement does not need to be done inline with each test. Instead, a fan frequency–mass flow curve can be fitted during the calibration campaign. Re-calibration of this relationship may become necessary over time due to degradation of the fan, but in that case, the ANN approaches will also be affected.

3.4.4. Sensitivity analysis

A sensitivity analysis was performed using Sobol's technique. The results are different sensitivities indices such as total sensitivity indices (total-order), first-order sensitivity indices (frst-order), and interaction sensitivity indices (second-order). First-order measures the direct effect of an input variable on the output, excluding interaction effects with other variables, while the second-order measures specifically this interaction effects. Finally, total-order indices account for the total effect of an input variable, including both direct and interaction effects. In Fig. 12, only total-order sensitivity indices are represented in the y-axis for the two output variables (outlet temperature on the top and water consumption on the bottom). Its value ranges from 0 to 1, where 0 means the variable has no effect, and 1 means it has a significant effect on the output.[4] The x-axis represents the system's inputs and includes

[4] Values can go slightly above 1 due to computing errors. This is due to the Sobol' sequence sample generator producing some unfeasible test samples that need to be discarded.

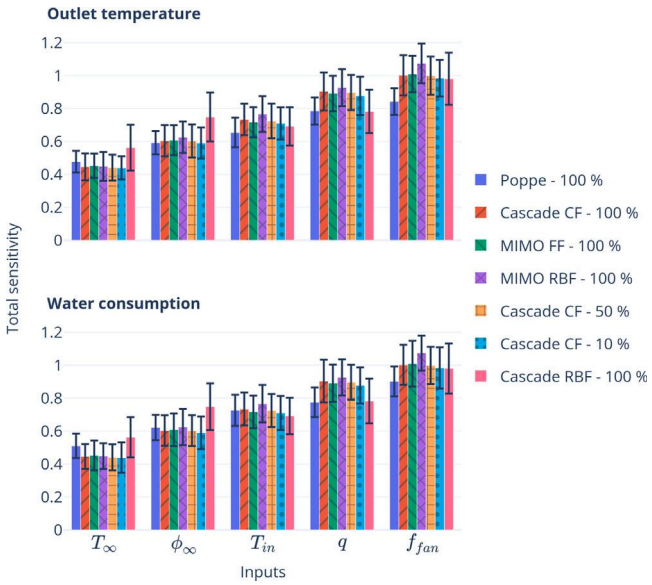

Fig. 12. Sobol's sensitivity analysis result for different case studies.

a bar for some of the obtained models with different calibration or training data points.

Comparing the results obtained for the different modelling approaches in Fig. 12, it can be seen that very homogeneous results are obtained in all cases, except for the Cascade RBF case, which was the worst performing of all the alternatives. These results serve to confirm that, at least from a sensitivity analysis point of view, all valid approaches are similarly sensitive to variations in the same inputs, which is desirable since they are trying to predict the same physical system. In the case of Cascade RBF, a discrepancy can be observed; less relevant input variables (T_{amb} and ϕ_∞) are overestimated and overall higher uncertainties in sensitivity are observed.

It is also important to highlight that the observed results are in agreement with the underlying physics of the heat and mass transfer processes occurring in the exchange area of the tower. The frequency of the fan and the volumetric flow rate are directly related to $\dot{m}_a$ and $\dot{m}_w$, respectively, and they have a high influence on the heat transfer coefficients. These coefficients govern the evaporation processes, which impact the evaporation rate (water lost due evaporation) and the outlet water temperature. On the other hand, the ambient conditions and the inlet water temperature also affect the outputs, but less significantly, since the driving force for the evaporation is the difference between the inlet air enthalpy and the enthalpy of saturated air evaluated at water temperature.

3.4.5. Scalability and performance in diverse operating and environment conditions

One important advantage of the Poppe model is its adaptability to large scale systems, as long as the system configuration remains the same. This allows to study and analyse pilot scale plants and extrapolate the results to industrial sized plants.

In addition, this model is also capable of accurately predicting the behaviour of the WCT in conditions that have not been tested (different environmental conditions or inlet water temperatures). It would even be valid for unknown $\dot{m}_w/\dot{m}_a$, although the reliability of the model would be lower if this ratio moves away from those experimentally used for calibration. On the contrary, ANN models are only applicable to the system and operating ranges they are trained for. Even though there are techniques to create new ANN models from previously trained ones [29], this is not a straightforward issue and it would require expertise and additional experimental data.

3.4.6. Implementation

In the recent years and due to the increase popularity of artificial intelligence, there are many libraries of easy access for most common programming languages, which makes the development and implementation of ANN models achievable by non experts or specialized teams. The need of extensive data can be mitigated if an online steady-state identification is implemented [30], which allows updating the model with a growing dataset. In the case of the Poppe model, although the number of tests is not a problem, it is necessary to have a deep knowledge of psychrometrics and heat and mass transfer disciplines to handle the governing equations described in Section 2.3.1 and the variables involved. On the other hand, solving the system of differential equations requires a non linear solver, which nowadays it is not a concern since there is a wide variety of software tools and packages available.

3.4.7. Execution time

In the case of the ANN model, the execution time is very low (in the order of milliseconds) and it is independent on the input conditions. In the case of the Poppe model, it is larger as it depends on the non-linear solver used, and this in turn has a variable processing time depending on how far the solution is from the initial point. The execution time for each alternative in evaluating the entire validation dataset (Exp 3 consisting of 17 tests, see Section 2.4.3) is included in Table 4. All of these results were obtained running each alternative on the same hardware, an 11th Gen Intel Core i7-1165G7 with 16 GB of RAM.

In general, the ANN models take 0.004 s to complete the evaluation in the MIMO configuration, and about double for cascade configuration. This difference was expected since the cascade configuration is running two networks in series. Nonetheless, in both cases the execution time is very low, especially compared to the obtained 6.3 s (almost a factor of 10^3) for the same task with Poppe's implementation.

This significant advantage of the ANN alternative is partly due to how fast the computation of neural networks is, and also due to their vectorization capabilities. Evaluating a bigger set would not take significantly more time.

This issue can limit the use of the physical model in optimization applications such as the determination of optimal operating conditions to minimize the water consumption of combined cooling systems for CSP plants. In this kind of use-cases, iteration times of less than a second are required to make its implementation feasible.

4. Conclusions and final recommendations

This paper presents a thorough comparison between two modelling alternatives: artificial neural networks and Poppe physical model. It is applied to wet cooling towers when they are integrated into combined cooling systems, with the aim of optimizing this integration. The main conclusions obtained during the investigation and final recommendations can be summarized as follows:

Regarding the prediction of the output variables, in the case of the outlet water temperature, both models reported good results, with low errors falling within the uncertainty range of the experimental equipment. Nonetheless, the physical model performs better than the best ANN alternative (MIMO RBF): $R^2 = 0.98$ and RMSE = 0.33 °C compared to $R^2 = 0.95$ and RMSE = 0.51 °C, respectively.

For the predictions of water consumption, it was shown that the Poppe model accurately predicts this variable, with results of $R^2 = 0.97$ and RMSE = 8.47 l/h. The best ANN alternative (cascade CF) achieves close results with an $R^2 = 0.95$ and RMSE = 11.24 l/h.

However, the Poppe model reached such reliable prediction levels with a much lower number of tests, needing only 2. In comparison, the ANN alternatives need more data, at least 10 (with a good distribution over the operating range) for the FF and CF ANN models.

One of the main strengths of the Poppe model is its ability to predict the operation of the tower regardless of the conditions tested. This

model is recommended to be used when it is necessary to scale up to larger systems, as long as the system design remains the same. In the case of the ANN model, it is only applicable to the same conditions and the same tower for which the model was developed.

The ANN model also has several strengths compared to the Poppe model. The most important one is the lower execution time. The ANN model is faster by orders of magnitude, it can be vectorized and its execution time is more constant regardless of the input conditions, in the order of milliseconds. Another advantage is that it can be developed and implemented without knowledge of the physical processes that take place in a wet cooling tower.

Ultimately, the factor that determines which alternative to use is the application of the model. For applications where its feasibility does not depend strongly on execution time, the physical model provides good results with minimal experimental data requirements. However, if execution time is an important factor, then any of the ANNs alternatives shown in this work, or other alternative machine learning methods are worth exploring. In those cases where both fast execution times are required and few experimental data is available, a combination of the two strategies is recommended. In this scenario, an ANN could be trained using data generated by the physical model and then validated using the available experimental information.

For the case study objective, a novel combined cooling system coupled to a CSP plant, the model needs to be integrated into an optimization scheme, so execution times are a priority and the predictive capabilities of the ANNs alternatives are satisfactory. The authors' recommendation for this or similar applications is to use a cascade-forward ANN architecture in a cascade model configuration or a MIMO radial-basis, either trained using experimental data if available, or using data provided by the physical model.

As a final remark, the results and conclusions presented here should not be taken as absolute, but rather as a methodology to systematically and rigorously compare both techniques. The family of neural network architectures is large and ever-growing, with potential reduction of some of the weaknesses outlined here. In addition, machine learning methods such as Gaussian Process Regression [31], Random Forest [32], ensemble methods such as Gradient Boosting [32] or Support Vector Machines [33] could be further explored.

CRediT authorship contribution statement

Juan Miguel Serrano: Writing – review & editing, Writing – original draft, Visualization, Validation, Supervision, Software, Methodology, Investigation, Data curation, Conceptualization. **Pedro Navarro:** Visualization, Validation, Software, Investigation, Data curation, Conceptualization, Writing – original draft, Writing – review & editing. **Javier Ruiz:** Writing – review & editing, Writing – original draft, Validation, Supervision, Methodology, Conceptualization, Investigation. **Patricia Palenzuela:** Formal analysis, Funding acquisition, Investigation, Project administration, Supervision, Writing – original draft, Writing – review & editing. **Manuel Lucas:** Writing – review & editing, Supervision, Formal analysis. **Lidia Roca:** Conceptualization, Data curation, Formal analysis, Funding acquisition, Investigation, Methodology, Project administration, Supervision, Validation, Visualization, Writing – original draft, Writing – review & editing.

Declaration of competing interest

The authors declare that they have no known competing financial interests or personal relationships that could have appeared to influence the work reported in this paper.

Data availability

Both experimental data and source code to replicate the results (for the ANNs) are available in Zenodo http://dx.doi.org/10.5281/zenodo.10806200.

Acknowledgements

This publication is part of the R&D project PID2021-126452OA-I00, funded by MCIN/AEI/10.13039/501100011033/ and ERDF A way of making Europe. The authors thank the Plataforma Solar de Almeria for providing access to its installations.

References

[1] IEA. Energy technology perspectives. 2014, URL: https://www.iea.org/reports/energy-technology-perspectives-2014.
[2] Rezaei E, Shafiei S, Abdollahnezhad A. Reducing water consumption of an industrial plant cooling unit using hybrid cooling tower. Energy Convers Manage 2010;51(2):311–9. http://dx.doi.org/10.1016/j.enconman.2009.09.027.
[3] El Marazgioui S, El Fadar A. Impact of cooling tower technology on performance and cost-effectiveness of CSP plants. Energy Convers Manage 2022;258:115448. http://dx.doi.org/10.1016/j.enconman.2022.115448, URL: https://www.sciencedirect.com/science/article/pii/S0196890422002448.
[4] Barigozzi G, Perdichizzi A, Ravelli S. Wet and dry cooling systems optimization applied to a modern waste-to-energy cogeneration heat and power plant. Appl Energy 2011;88(4):1366–76. http://dx.doi.org/10.1016/j.apenergy.2010.09.023.
[5] Barigozzi G, Perdichizzi A, Ravelli S. Performance prediction and optimization of a waste-to-energy cogeneration plant with combined wet and dry cooling system. Appl Energy 2014;115:65–74. http://dx.doi.org/10.1016/j.apenergy.2013.11.024.
[6] Palenzuela P, Roca L, Asfand F, Patchigolla K. Experimental assessment of a pilot scale hybrid cooling system for water consumption reduction in CSP plants. Energy 2022;242:122948. http://dx.doi.org/10.1016/j.energy.2021.122948.
[7] Asfand F, Palenzuela P, Roca L, Caron A, Lemarié C-A, Gillard J, Turner P, Patchigolla K. Thermodynamic performance and water consumption of hybrid cooling system configurations for concentrated solar power plants. Sustainability 2020;12(11). http://dx.doi.org/10.3390/su12114739, Number: 4739.
[8] Wazirali R, Yaghoubi E, Abujazar MSS, Ahmad R, Vakili AH. State-of-the-art review on energy and load forecasting in microgrids using artificial neural networks, machine learning, and deep learning techniques. Electr Power Syst Res 2023;225:109792. http://dx.doi.org/10.1016/j.epsr.2023.109792, URL: https://www.sciencedirect.com/science/article/pii/S0378779623006818.
[9] Merkel F. Verdunstungskühlung. Berlin, Alemania: VDI Zeitschriff Deutscher Ingenieure; 1925, p. 123–8, tex.volumen: 70.
[10] Bourillot C. Hypotheses of calculation of the water flow rate evaporated in a wet cooling tower. 1983, Place: United States.
[11] Jaber H, Webb RL. Design of cooling towers by the effectiveness-NTU method. J Heat Transfer 1989;111(4):837–43. http://dx.doi.org/10.1115/1.3250794.
[12] Poppe M, Rögener H. Berechnung von rückkühlwerken. In: VDI wärmeatlas. 1991, p. Mi 1.
[13] Kloppers J, Kröger D. A critical investigation into the heat and mass transfer analysis of counterflow wet-cooling towers. Int J Heat Mass Transfer 2005;48(3):765–77. http://dx.doi.org/10.1016/j.ijheatmasstransfer.2004.09.004, URL: https://www.sciencedirect.com/science/article/pii/S0017931004004041.
[14] Cutillas CG, Ruiz J, Asfand F, Patchigolla K, Lucas M. Energetic, exergetic and environmental (3E) analyses of different cooling technologies (wet, dry and hybrid) in a CSP thermal power plant. Case Stud Therm Eng 2021;28:101545. http://dx.doi.org/10.1016/j.csite.2021.101545, URL: https://www.sciencedirect.com/science/article/pii/S2214157X21007085.
[15] Hosoz M, Ertunc HM, Bulgurcu H. Performance prediction of a cooling tower using artificial neural network. Energy Convers Manage 2007;48(4):1349–59. http://dx.doi.org/10.1016/j.enconman.2006.06.024.
[16] Gao M, Shi Y-t, Wang N-n, Zhao Y-b, Sun F-z. Artificial neural network model research on effects of cross-wind to performance parameters of wet cooling tower based on level Froude number. Appl Therm Eng 2013;51(1):1226–34. http://dx.doi.org/10.1016/j.applthermaleng.2012.06.053.
[17] Song J, Chen Y, Wu X, Ruan S, Zhang Z. A novel approach for energy efficiency prediction of various natural draft wet cooling towers using ANN. J Therm Sci 2021;30(3):859–68. http://dx.doi.org/10.1007/s11630-020-1296-0.
[18] Nossent J, Elsen P, Bauwens W. Sobol'sensitivity analysis of a complex environmental model. Environ Model Softw 2011;26(12):1515–25, Publisher: Elsevier.
[19] Herman J, Usher W. SALib: An open-source python library for sensitivity analysis. J Open Source Softw 2017;2(9). http://dx.doi.org/10.21105/joss.00097, Publisher: The Open Journal.
[20] Iwanaga T, Usher W, Herman J. Toward SALib 2.0: Advancing the accessibility and interpretability of global sensitivity analyses. Soc-Environ Syst Model 2022;4:18155. http://dx.doi.org/10.18174/sesmo.18155, URL: https://sesmo.org/article/view/18155.
[21] Navarro P, Ruiz J, Hernández M, Kaiser A, Lucas M. Critical evaluation of the thermal performance analysis of a new cooling tower prototype. Appl Therm Eng 2022;213:118719. http://dx.doi.org/10.1016/j.applthermaleng.2022.118719.

[22] Ashrae. HVAC systems and equipment. In: Chapter 36 cooling towers. 2004.
[23] Hagan MT, Demuth HB, Beale MH, Jesús OD. Neural network design. Martin Hagan; 2014.
[24] Beale MH, Hagan MT, Demuth HB. Neural network toolbox. Vol. 2, User's Guide, MathWorks; 2010, p. 77–81.
[25] Hamm L, Brorsen BW, Hagan MT. Comparison of stochastic global optimization methods to estimate neural network weights. Neural Process Lett 2007;26(3):145–58. http://dx.doi.org/10.1007/s11063-007-9048-7, URL: https://doi.org/10.1007/s11063-007-9048-7.
[26] UNE. Thermal performance acceptance testing of mechanical draft series wet cooling towers. Manual, UNE; 2004.
[27] CTI. Code tower, standard specifications. Acceptance test code for water cooling towers. Manual, Cooling Technology Institute; 2000.
[28] Ruiz J, Navarro P, Hernández M, Lucas M, Kaiser A. Thermal performance and emissions analysis of a new cooling tower prototype. Appl Therm Eng 2022;118065. http://dx.doi.org/10.1016/j.applthermaleng.2022.118065, URL: https://www.sciencedirect.com/science/article/pii/S135943112200031X.
[29] Zhuang F, Qi Z, Duan K, Xi D, Zhu Y, Zhu H, Xiong H, He Q. A comprehensive survey on transfer learning. Proc IEEE 2020;109(1):43–76, Publisher: IEEE.
[30] Pérez-Sánchez B, Fontenla-Romero O, Guijarro-Berdiñas B. A review of adaptive online learning for artificial neural networks. Artif Intell Rev 2018;49:281–99, Publisher: Springer.
[31] Rasmussen CE, Williams CKI. Gaussian processes for machine learning. Adaptive computation and machine learning, Cambridge, Mass: MIT Press; 2006, OCLC: ocm61285753.
[32] Breiman L. Random Forests. Mach Learn 2001;45(1):5–32. http://dx.doi.org/10.1023/A:1010933404324.
[33] Steinwart I, Christmann A. Support vector machines. Springer Science & Business Media; 2008, Google-Books-ID: HUnqnrpYt4IC.